

Evidence for a Possible Proton-Antiproton Bound State from Lattice QCD

Muhammad Ushtaq Loan

Department of Physics, Zhongshan University, Guangzhou 510275, China.
School of Physics, The University of New South Wales, Sydney, NSW 2052, Australia
(Dated: May 25, 2019)

We have used standard techniques of lattice quantum chromodynamics to look for evidence of the spin-zero six quark flavor singlet state ($J^{PC} = 0^+$) observed by BES Collaboration, and to determine the splitting between the mass of the possible proton-antiproton and the mass of two protons, its threshold. Ignoring quark loops and quark annihilation, we find indications that for sufficiently light quarks proton-antiproton is below the $2m_p$ threshold, making it a possible six-quark bound state.

PACS numbers: 11.15.Ha, 12.38.Gc, 11.15.Me

Recently, the BES Collaboration in Beijing observed a near threshold enhancement in the proton-antiproton (pp) mass spectrum from $J=1^-$ pp radiative decay [1]. Fitting the enhancement with an S -wave Breit-Wigner resonance function, results in peak mass at $M = 1859^{+3}_{-10}(\text{stat})^{+5}_{-25}(\text{sys})$ with a total width < 30 MeV = c^2 . With a P -wave fit, the peak mass is very close to the threshold, $M = 1876.4 \pm 0.9$ MeV and the total width is very narrow, $= 4.6 \pm 1.8$ MeV. This discovery is subsequently confirmed by the Belle Collaboration in different reactions of the decays $B^+ \rightarrow K^+ pp$ [2] and $B^0 \rightarrow D^0 pp$ [3], showing enhancements in the pp invariant mass distribution near $2m_p$. Such a mass and width does not match that of any known particle [4].

Theoretically existence of such a state was predicted using quark model and conventional nucleon potentials [5, 6, 7, 8]. However, a prediction closest in mass and width with the experiment was made recently by Yan et al using the Skyrme model [9]. Experimentally, spin, parity and isospin of pp (1857) are not well determined yet. The photon polar angle distribution was found consistent with $1 + \cos^2 \theta$ suggesting the angular momentum is very likely to be $J = 0$. Making full use of general symmetry requirement and available experimental information the corresponding spin and parity are $J^{PC} = 0^+$ [10]. In this letter we report first quenched lattice QCD calculation capable of studying the pp (1859).

It is not easy to deal with $q^m q^n$ ($m + n = 3$) states rather than conventional baryons and mesons in lattice QCD. For example, a $q^3 q^3$ state can be decomposed into couple of colour singlets states even in the quenched approximation. The two-point function, in general, couples not only to the single hadron but also to the two-hadron states. If one allows such transitions, then - much like pentaquarks - it is not easy to separate and analyze the spectrum. In this study, we shall restrict ourselves to a 6-quark exotic with no transitions to regular mesons. We seek an operator that has a little overlap with the hadronic two-body states in order to identify the signal of our hexaquark state in lattice QCD. For this purpose, we propose a local operator based on the description of

diquarks.

In Jade model [11], each pair of $[ud]$ form a diquark which transforms like a spin singlet (1_s), colour anti-triplet (3_c), and the flavor anti-triplet (3_f).

$$Q^{i;a}(x) = \frac{1}{2} \epsilon_{ijk} \epsilon_{abc} q_{j;b}^T(x) C q_{k;c}(x); \quad (1)$$

where C is the charge conjugation matrix, abc the colour indices, and ijk the flavor indices. The Dirac structure of the operator is represented by the matrices γ , satisfying $\gamma^2 = 1$ such that the diquark operator transforms like a scalar or pseudoscalar. Accounting for both colour and flavor antisymmetries, possible γ are restricted within 1 and 5. Then the hexaquark hadron $pp([ud][ud][uu])$ emerges as a member with $S = 0$ and $I = 0$ in $(Q^3 \otimes Q^3) \otimes Q^6 = ([15_{cs}] \otimes [15_{cs}]) \otimes [21_{cs}]$ in SU(6) colour-spin representation and a flavor singlet in $(3_f \otimes 3_f) \otimes 6_f$. With this picture the local interpolating operator for pp is obtained as

$$O_{pp}(x) = \epsilon_{abc} Q^{i;a}(x) Q^{j;b}(x) Q^{k;c}(x) \quad (2)$$

where $Q^0 = u^T C^{-1} \epsilon_{5}^{00} u$. This identification looks familiar if we represent one of the quarks by charge conjugate field: $q_a q_b \rightarrow q_a q_b^*$, where $q_b^* = i q_b^T \epsilon_{5}^{00}$. Then the classification of diquark bilinears is analogous to that of qq bilinears. We choose $\gamma = 1$ and $\gamma^0 = \gamma^{\infty} = 5$. There are many more possibilities of constructing the operator even in the $I = 0$ channel. In principle testing other interpolating operators and checking which one has the best overlap with pp state should provide information on the wave function of the particle. In this study, however, we do not pursue this direction any further. It is worth mentioning that with our proposed operator the description does not rely on highly correlated diquarks and it is straightforward to work out the hadron propagators in terms of quark propagators.

To examine the pp in lattice QCD, we generate quenched configurations a $16^3 \times 48$ lattice with tadpole-improved anisotropic gluon action [12] at $\beta = 2.4$ 3.2, which correspond to lattice spacings of 0.48 0.37 fm. Gauge configurations are generated by a 5-hit

pseudo heat bath update supplemented by four over-relaxation steps. These configurations are then fixed to the Coulomb gauge at every 500 sweeps. After discarding the initial sweeps, a total of 300 configurations for each κ_t are accumulated for measurements. Using the tadpole-improved clover quark action on the anisotropic lattice [13] we compute the light-quark propagators at six values of the hopping parameter κ_t for bare quark mass in the range 10 – 100 MeV. We adopt a bin size of 30 configurations.

To perform precise parity projection, we construct forward propagating quarks by taking the appropriate linear combination of propagators with periodic and anti-periodic boundary conditions in spatial and time directions respectively. This procedure yields a signal at large Euclidean times which is crucial for the calculation. Hadron masses are obtained from the correlation functions of multi-quark operators having the same quantum numbers as the hadrons in question. To obtain a better overlap with the ground state we used iterative smearing of gauge links and the application of the fuzzing technique for the fermion fields [14]. The application of fuzzing for two of the six quarks inside the pp attens the curvature of the effective mass. The largest plateau in the region with small errors is obtained with fussed u- and d-quarks. We used this variant to calculate our correlation functions.

From the correlation functions we extract them ass (energy) by standard χ^2 fitting with multi-hyperbolic cosine ansatz

$$C(t) = \sum_{i=1}^{N_c} A_i \cosh(t m_i) \quad (3)$$

The purpose of using the multi-state t is to reduce the contamination from excited states. The fitting range $[t_{m_{in}}; t_{m_{ax}}]$ for the final analysis is determined by fixing $t_{m_{ax}}$ and finding a range of $t_{m_{in}}$ where the ground state mass is stable against $t_{m_{in}}$. We choose one "best t " which is insensitive to the t range, has high confidence level and reasonable statistical errors. Typical example of the effective mass plot is shown in Fig. 1. An impressive plateau with reasonable statistical errors is seen to terminate at $t = 40$. The 2-cosh t for pp state gives the ground state mass consistent with that from 1-cosh t . Statistical errors of masses are estimated by a single elimination jackknife method. We kept statistical errors under control by ensuring that analyzed configurations are uncorrelated, which is made possible by separating them by as many as 500 sweeps. The statistical uncertainties on our hadron masses are typically on the few percent level. In addition to the pp state we calculated the masses of the non-strange mesons, as well as the nucleon. These particle masses were used for scale setting and analyzing the stability of pp state, respectively.

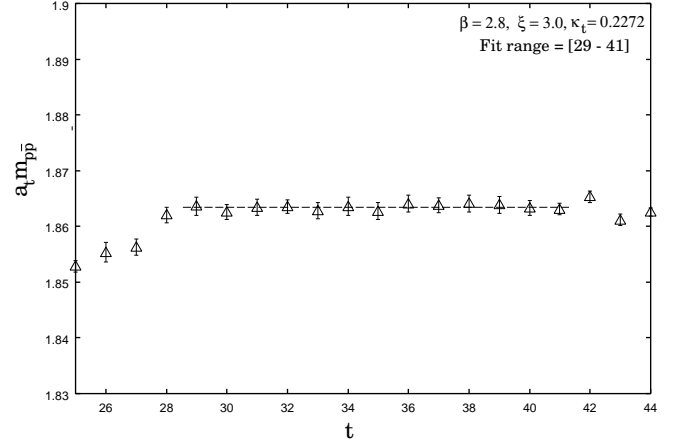


FIG. 1: Effective mass of pp state as a function of $t_{m_{in}}$. The dashed line represents fitted mass and its statistical errors.

Fig. 2 collects and displays the resulting particle masses extrapolated to the physical quark mass value using linear and quadratic fits. The difference between the two extrapolations gives some information about systematic uncertainties in the extrapolated quantities. Although, our quark masses are quite small and we have only five different quark masses at each κ_t , both linear and quadratic fits essentially gave the identical results. We believe that the uncertainties due to chiral logarithms in the physical limit are subdominant at our present statistics. However, since quenched spectroscopy is quite reliable for mass ratio of stable particles, it is physically even more motivated to extrapolate mass ratio instead of mass. Fig. 3 shows the chiral extrapolation of the pp to nucleon mass ratio at two different lattice sizes. It can be seen that quark mass dependence of this ratio seems to be weaker than individual hadrons (Fig. 2). Although our spatial lattice size is big enough for treating our measurements without finite-size effects, a finite-size consistency check was done on a $12^3 \times 36$ lattice at $\kappa_t = 3.0$. With our statistical errors of order a few percent we did not find the size dependence in the hadron masses and mass ratios. The finite-size uncertainty in our quenched analysis turned out to be less than 0.2% for the pp ground state and less than 0.1% for the nucleon.

The major source of discrepancy among the lattice spacings from different observables is the quenching effect. The obtained π and N masses are compared to the experimental values and show a deviation less than 4–6% for the lattice sizes explored here. Such a variance can be considered as usual quenching effect. Of course, simulations with dynamical fermions might be useful to eliminate this error all together. Inspired by the good agreement of the π and N masses with their experimental values, the scale was set by the π mass. We included a modest estimate of 5% quenching uncertainty in our analysis.

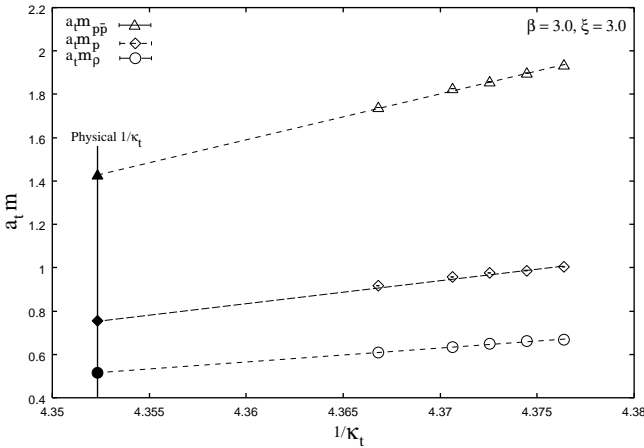


FIG. 2: Chiralextrapolation of hadron masses on one of our nest lattices.

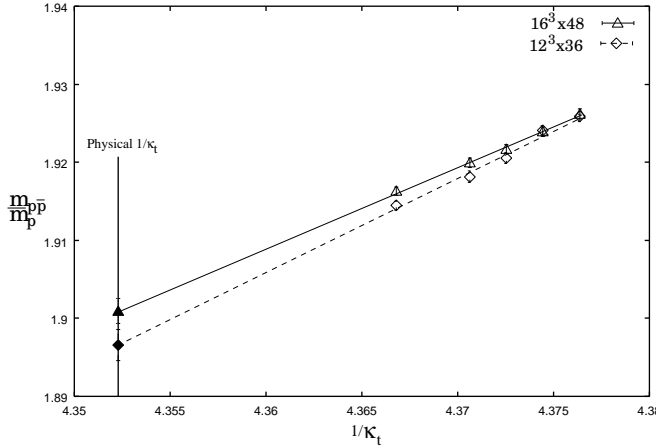


FIG. 3: Chiralextrapolation of the mass ratio on two different lattice sizes at $\beta = 3.0$.

Finally, we performed a continuum extrapolation for the chirally extrapolated quantities in Fig. 4. The possible error that might effect the simulation results comes from the scaling violation for our actions. Expecting that dominant part of scaling violation errors is largely eliminated by tadpole improvement, we extrapolate the results at finite a_s to the continuum limit $a_s \rightarrow 0$. Here we adopt an a_s^2 -linear extrapolation for the continuum limit, because the leading order scaling violation for our fermion action is $O(a_s^2 QCD m_q)$. We also perform an a_s -linear extrapolation to estimate systematic errors. In practice we use results at four nest lattice spacings, i.e.,

$\beta = 2.6 - 3.2$ for the continuum extrapolation, excluding results at $\beta = 2.4$, which appear to have larger discretization errors as expected from the naive order estimate. Performing such extrapolations, we adopt the choice which shows the smoothest scaling behaviour for the final value, and use others to estimate the systematic errors. As can be seen from Fig. 4, the mass ratio

again shows a weak dependence on the lattice spacing and varies only slightly over the fitting range. The four non-zero lattice spacing values of the ratio are within $0.04 - 0.06$ standard deviations of the extrapolated zero lattice spacing result. This will make for unambiguous and accurate continuum extrapolation. Given the fact that the ratio does not show any scaling violations, we could also quote the value of this quantity on our nest lattice, which has the smallest error. Nevertheless, order 7% errors on the finally quoted values are mostly due to the chiral and the continuum extrapolation. The continuum results obtained are summarized in Table I. Using

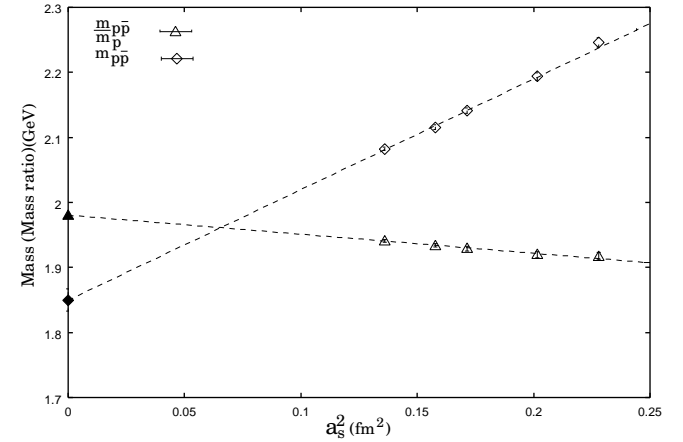


FIG. 4: Continuum extrapolation of the pp mass and the mass ratio m_{pp}/m_p . The dashed lines are linear fits to the data in the range $0.136 < a_s^2 < 0.2015$. Solid symbols represent the predicted continuum values.

the physical nucleon mass $m_p = 938$ MeV, we obtain a continuum mass estimate of 1859 ± 16 MeV for the pp. Although the extrapolation of m_{pp} to the continuum limit shows significant discretization errors, the results from two extrapolations seem to be in good agreement, within errors. The lowest mass that we find in $J^{PC} = 0^+$ channel is in complete agreement with the experimental value of pp mass [1]. The known isosinglet X (1860) is obvious candidate to identify with the pp bound state we seem to have found on the lattice.

Now all prerequisites are available to investigate the stability of pp state. To eliminate some of the statistical uncertainties we analyzed directly the ratio of correlators of the pp and the nucleon. This ratio is expected to take the single exponential form only at large t after contributions from excited states have died away. Following the usual procedure of looking for a plateau, we measured the binding energy E for several different lattice spacings. It is clear from Fig. 5 that the binding energy is varying rather slowly in the lattice spacing and we expect that this will lead to a bound state in the infinite volume limit. Note, that our continuum extrapolated $m_{pp}/2m_p$ is merely an illustration. Adopting an a_s^2 -linear extrap-

TABLE I: Chirally extrapolated results at finite lattice spacings. The continuum limit predictions were obtained by extrapolating the data for hadron masses as well as the mass ratio.

a_s^2 (fm $^{-2}$)	m_p (GeV)	m_{pp} (GeV)	$m_{pp} = m_p$	m_{pp} (GeV)	$2m_p$ (GeV)	E (GeV)
0.2279	1.191 (5)	2.277 (7)	1.917 (6)	-0.106 (4)	0.075 (4)	
0.2015	1.143 (5)	2.193 (6)	1.919 (4)	-0.093 (4)	0.069 (3)	
0.1715	1.113 (3)	2.140 (4)	1.929 (4)	-0.086 (3)	0.064 (3)	
0.1578	1.098 (3)	2.115 (3)	1.934 (3)	-0.082 (2)	0.058 (2)	
0.1360	1.080 (2)	2.085 (3)	1.941 (2)	-0.074 (2)	0.053 (1)	
! 0	0.947 (13)	1.851 (24)	1.982 (17)	-0.018 (2)	0.016 (2)	

olation we obtain a continuum result which implies that pp state does indeed move into the continuum as a bound state with a binding energy of 16–18 MeV.

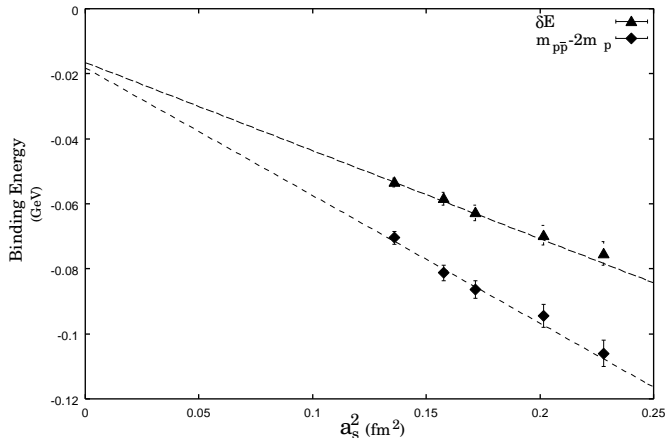


FIG. 5: Continuum extrapolation of the binding energy.

Our estimates show a good agreement with the corresponding binding energies obtained in the potential model [9] and the experimental results [1]. The behaviour of the bound state in this potential model is not meant to be definitive but it illustrates the expected behaviour of a pp bound state: tracking m_{pp} with roughly constant binding energy as m_p falls.

We have presented the results of the first lattice investigation on the pp state employing improved gauge and fermion anisotropic actions, relatively light quark masses as well as smearing and fuzzing techniques to enhance the overlap with the ground state of the particle. Our analysis takes into account all possible uncertainties, such as statistical, finite-size, and quenching errors when performing the chiral and continuum extrapolations. On

the basis of our lattice calculation we speculate that the state is to be identified as the continuum relic of bound state of six quarks. However, a thorough examination of this question would require the implementation of flavour SU(3) violation. The $I = 0$ pp state couples to 4 [10] through the ss component of the in the quenched approximation. By giving the strange quark a larger mass would alter threshold which in turn would affect the manifestation of the bound state. Calculations on lattice with variation with quark mass are needed to confirm our results. Although it seems natural to expect that for sufficiently heavy quarks a bound state will remain, but only full, unquenched lattice calculations can confirm this. We did not make a systematic study of possible interpolating operators that are likely to have good overlap with pp. This study would be also important. We plan to further develop this calculation to involve more interpolating operators.

I would like to thank R. Jaffe, C. Michael, C. Detar, C. Hammer and D. Leinweber for valuable suggestions. It is a pleasure to acknowledge Shan Jin for his hospitality at CCAST and stimulating discussions. The computations were carried on the 64 node CS cluster of Computer Center, using a modified version of the publicly available MILC code (see www.physics.indiana.edu/sg/milc.html). This work was supported by the Guangdong Provincial Ministry of Education.

-
- [1] J.Z. Bai et al., Phys. Rev. Lett. 91 022001 (2003)
 - [2] K. Abe et al., Phys. Rev. Lett. 88 181803 (2002)
 - [3] K. Abe et al., Phys. Rev. Lett. 89 151802 (2002)
 - [4] Particle Data Group, Phys. Rev. D 66, 010001 (2002)
 - [5] E. Kempton, F. Bradamante, A. Martin and J.-M. Richard, Phys. Rep. 368, 119 (2002)
 - [6] J.-M. Richard, Nucl. Phys. B (Proc. Suppl.) 86, 361 (2000)
 - [7] A. Datta and O'Donnell, Phys. Lett. B 567, 273 (2003)
 - [8] J.L. Rosner, Phys. Rev. D 68, 014004 (2003)
 - [9] Mu-Lin Yan, SiLi, Bin Wu and Bo-Qiang Ma, Phys. Rev. D 72, 034027 (2005)
 - [10] Chong-Shou Gao and Shi-Lin Zhu, Commun. Theor. Phys. 42, 844 (2004)
 - [11] R.L. Jaffe, Phys. Rev. D 15, 281 (1977)
 - [12] C.J. Morningstar and M.J. Peardon, Phys. Rev. D 60, 034509 (1999)
 - [13] M. Okamoto, et al., [CP-PACS Collaboration], Phys. Rev. D 65, 094508 (2002)
 - [14] P. Lacock et al., [UKQCD Collaboration], Phys. Rev. D 51, 6403 (1995)